

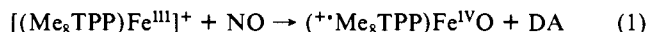
# The Kinetics and Mechanisms of Oxygen Transfer in the Reaction of *p*-Cyano-*N,N*-dimethylaniline *N*-Oxide with Metalloporphyrin Salts. 4.<sup>1</sup> Catalysis by *meso*-(Tetrakis(2,6-dimethylphenyl)porphinato)iron(III) Chloride

T. C. Woon, C. Michael Dicken, and Thomas C. Bruice\*

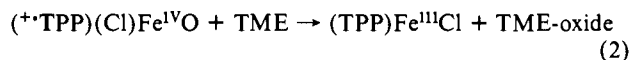
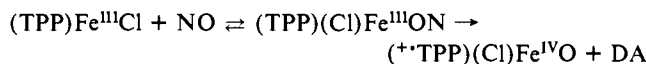
Contribution from the Department of Chemistry, University of California at Santa Barbara, Santa Barbara, California 93106. Received June 23, 1986

**Abstract:** *meso*-(Tetrakis(2,6-dimethylphenyl)porphinato)iron(III) chloride ((Me<sub>8</sub>TPP)Fe<sup>III</sup>Cl) is a catalyst for the conversion of *p*-cyano-*N,N*-dimethylaniline *N*-oxide (NO) to *p*-cyano-*N,N*-dimethylaniline (DA), *p*-cyano-*N*-methyl-aniline (MA), *p*-cyano-*N*-formyl-*N*-methyl-aniline (FA), *p*-cyanoaniline (A), *N,N'*-dimethyl-*N,N'*-bis(*p*-cyanophenyl)hydrazine (H), *N,N'*-bis(*p*-cyanophenyl)-*N*-methylmethylenediamine (MD), and CH<sub>2</sub>O. All evidence supports these reactions to occur by equilibrium ligation of NO to iron(III) porphyrin followed by rate-determining oxygen transfer to yield as immediate products DA and the iron(IV)-oxo porphyrin  $\pi$ -cation radical. Stepwise oxidation of DA by the higher valent iron-oxo porphyrin species is responsible for the formation of the other products (i.e., DA  $\rightarrow$  FA, DA  $\rightarrow$  MA  $\rightarrow$  A, 2MA  $\rightarrow$  MD, and 2MA  $\rightarrow$  H). The oxidation potentials of (Me<sub>8</sub>TPP)Fe<sup>III</sup>OCH<sub>3</sub> are comparable to those of the unsubstituted *meso*-(tetraphenylporphinato)iron(III) methoxide ((TPP)Fe<sup>III</sup>OCH<sub>3</sub>). The following results are, therefore, not surprising: (i) The second-order rate constant ( $k_a k_b / k_a$ ) for reaction of (Me<sub>8</sub>TPP)Fe<sup>III</sup>Cl with NO is but 3.3-fold smaller than in the case of the reaction of NO with (TPP)Fe<sup>III</sup>Cl; (ii) the percentage yields of products (DA, 53%; MA, 24%; A, 3%; FA, 8%; H, 7%; MD, 5%) are comparable to when (TPP)Fe<sup>III</sup>Cl is employed; and (iii) oxidation and epoxidation of added substrates are not rate-determining. Of considerable interest is the finding that epoxidation reactions using NO with (Me<sub>8</sub>TPP)Fe<sup>III</sup>Cl occur in much higher yield (80% to 100%) than when (TPP)Fe<sup>III</sup>Cl is used as the catalyst.

Iron(III) porphyrins and manganese(III) porphyrins serve as catalysts in the conversion of *N,N*-dimethylaniline *N*-oxides to an *N*-methyl-aniline, and a host of its oxidation products, and to formaldehyde.<sup>1a</sup> The mechanism of this reaction has been established with *p*-cyano-*N,N*-dimethylaniline *N*-oxide (NO) and *meso*-(tetraphenylporphinato)iron(III) chloride ((TPP)Fe<sup>III</sup>Cl) to involve formation of *p*-cyano-*N,N*-dimethylaniline (DA) on transfer of oxygen from NO to the iron(III) porphyrin.<sup>1b,d</sup> Transfer of an oxygen atom to an iron(III) porphyrin involves 2e<sup>-</sup> oxidation of the iron(III) porphyrin. Spectroelectrochemical studies have established that 2e<sup>-</sup> oxidation of iron(III)-oxo porphyrins provide iron(IV)-oxo porphyrin  $\pi$ -cation radicals.<sup>2</sup> It is reasonable to assume, therefore, that oxygen transfer from NO to iron(III) porphyrin provides DA + iron(IV)-oxo porphyrin  $\pi$ -cation radical (eq 1). That oxygen transfer from *N*-oxide to

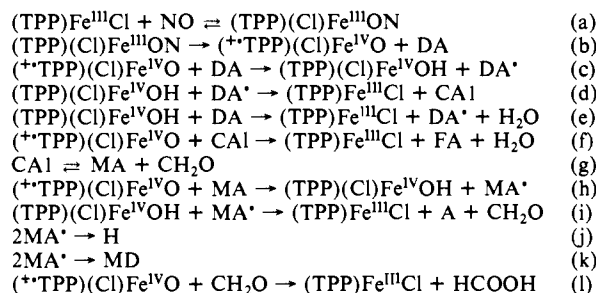


iron(III) porphyrin is rate determining was established by the comparison of the intermolecular (*p*-CNC<sub>6</sub>H<sub>4</sub>N<sup>+</sup>(CH<sub>3</sub>)<sub>2</sub>O<sup>-</sup>/(*p*-CNC<sub>6</sub>H<sub>4</sub>N<sup>+</sup>(CD<sub>3</sub>)<sub>2</sub>O<sup>-</sup>) and intramolecular discriminatory (*p*-CNC<sub>6</sub>H<sub>4</sub>N<sup>+</sup>(CH<sub>3</sub>)(CD<sub>3</sub>)O<sup>-</sup>) isotope effects and also by comparison of turnover rate constants when quantitatively trapping the iron(IV)-oxo porphyrin  $\pi$ -cation radical with 2,4,6-tri-*tert*-butylphenol (TBPH) or 2,3-dimethyl-2-butene (TME) (eq 2).<sup>1d</sup> Under trapping conditions with TBPH and TME, DA is recoverable in 100% yield based upon the initial concentration of



NO. In the absence of trapping agents the iron(IV)-oxo porphyrin

## Scheme I



$\pi$ -cation radical enters into a host of oxidations (Figure 1 and Scheme I) to provide *p*-cyano-*N*-methyl-aniline (MA), *p*-cyano-*N*-formyl-*N*-methyl-aniline (FA), *N,N'*-dimethyl-*N,N'*-bis(*p*-cyanophenyl)hydrazine (H), *N,N'*-bis(*p*-cyanophenyl)-*N*-methylmethylenediamine (MD), *p*-cyanoaniline (A), and formaldehyde. These oxidations must be initiated by reaction of the iron(IV)-oxo porphyrin  $\pi$ -cation radical with DA. Further work showed that FA, H, MD, and A were end products with all but FA coming from the oxidation of MA by the iron(IV)-oxo porphyrin  $\pi$ -cation radical. From the kinetics of products formation and a knowledge of the rate constant for the commitment step of oxygen transfer from NO to iron(III) porphyrin (obtained from the trapping experiments) we were able, through the use of computer simulation, to assign rate constants to the reactions of Scheme I.

The influence of electronic and steric factors in determining the time course and products of the reaction of NO with iron(III) porphyrins was initiated in a detailed investigation of the reaction of the more electron-deficient *meso*-(tetrakis(2,6-dichlorophenyl)porphinato)iron(III) chloride ((Cl<sub>8</sub>TPP)Fe<sup>III</sup>Cl) with NO.<sup>1e</sup> The reaction of NO with (TPP)Fe<sup>III</sup>Cl and (Cl<sub>8</sub>TPP)Fe<sup>III</sup>Cl may be compared. Only with the latter is there formed both mono- and bis-NO complexes. Formation of the mono-NO complex is thermodynamically much more favorable with (Cl<sub>8</sub>TPP)Fe<sup>III</sup>Cl than with (TPP)Fe<sup>III</sup>Cl. Also, oxygen transfer from N $\rightarrow$ Fe<sup>III</sup> within the mono-complex and oxidation of *p*-cyano-*N,N*-dimethylaniline by the resultant iron(IV)-oxo porphyrin  $\pi$ -cation

(1) (a) Shannon, P.; Bruice, T. C. *J. Am. Chem. Soc.* **1981**, *103*, 4500. (b) Nee, M. W.; Bruice, T. C. *Ibid.* **1982**, *104*, 6123. (c) Powell, M. F.; Pai, E. F.; Bruice, T. C. *Ibid.* **1984**, *106*, 3277. (d) Dicken, C. M.; Lu, F.-L.; Nee, M. W.; Bruice, T. C. *Ibid.* **1985**, *107*, 5776. (e) Dicken, C. M.; Woon, T. C.; Bruice, T. C. *Ibid.* **1986**, *108*, 1636.

(2) (a) Lee, W. A.; Calderwood, T. S.; Bruice, T. C. *Proc. Natl. Acad. Sci. U.S.A.* **1985**, *82*, 4301. (b) Calderwood, T. S.; Lee, W. A.; Bruice, T. C. *J. Am. Chem. Soc.* **1985**, *107*, 8272.

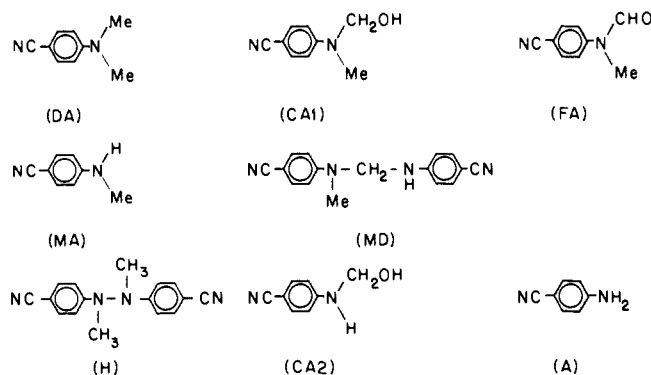


Figure 1. Amine products on reaction of NO with  $(\text{Me}_8\text{TPP})\text{Fe}^{\text{III}}\text{Cl}$ .

radical are much more facile (minimally  $10^3$ -fold) for the octachloro analogue. Though  $(\text{TPP})\text{Fe}^{\text{III}}\text{Cl}$  epoxidation yields with either NO or PhIO are comparable,  $(\text{Cl}_8\text{TPP})\text{Fe}^{\text{III}}\text{Cl}$  is a very poor catalyst for epoxidations with NO. Though  $(\text{Cl}_8\text{TPP})\text{Fe}^{\text{III}}\text{Cl}$  reacts quite rapidly with NO the octachloro iron(IV)-oxo  $\pi$ -cation radical which is formed has a greater propensity to oxidize the DA generated in the reaction than to epoxidize alkenes.

There is described herein a study of the reaction of NO with *meso*-(tetrakis(2,6-dimethylphenyl)porphinato)iron(III) chloride  $(\text{Me}_8\text{TPP})\text{Fe}^{\text{III}}\text{Cl}$ . We have previously<sup>2</sup> compared the CV redox

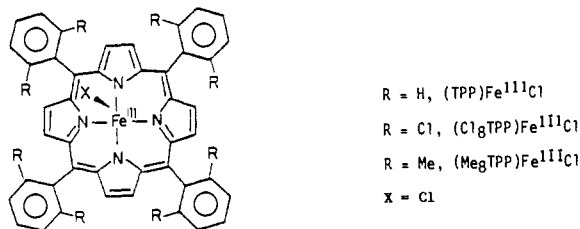


Figure 2. Plots of  $A_{320}$  vs. time for the  $(\text{Me}_8\text{TPP})\text{Fe}^{\text{III}}\text{Cl}$ -catalyzed decomposition of NO (where the  $[(\text{Me}_8\text{TPP})\text{Fe}^{\text{III}}\text{Cl}]_i = 8.0 \times 10^{-5}$  M and the  $[\text{NO}]_i$  was varied from  $8.0 \times 10^{-4}$  to  $8.0 \times 10^{-3}$  M) showing that the initial rates are dependent on the  $[\text{NO}]_i$ . Points are experimental and the lines computer generated from the first-order rate law.

H), 8.18 (s, 4 H), 14.22 (s, 4 H), 15.80 (s, 4 H), 80.41 (br s, 8 H); visible spectrum (molar absorptivity,  $\text{M}^{-1} \text{cm}^{-1}$ ) 377 ( $5.88 \times 10^4$ ), 418 ( $1.05 \times 10^5$ ), 510 ( $1.38 \times 10^4$ ), 576 ( $3.93 \times 10^3$ ), 660 ( $3.00 \times 10^3$ ), 695 ( $3.20 \times 10^3$ ); mass spectrum,  $m/z$ , ...  $[\text{M}]^+$  815,  $[\text{M} - \text{Cl}]^+$  (base peak) 780;  $[\text{M} - \text{Cl} - \text{C}_8\text{H}_{10}]^+$  674. *meso*-(Tetrakis(2,6-dimethylphenyl)porphinato)iron(III) hydroxide  $(\text{Me}_8\text{TPP})\text{Fe}^{\text{III}}\text{OH}$  was a sample from a previous study.<sup>7</sup> *p*-Cyano-*N,N*-dimethylaniline *N*-oxide (NO) was prepared as previously described.<sup>1d</sup> Alkenes were purchased from Aldrich. 2,3-Dimethyl-2-butene (TME), cyclohexene, styrene, cyclopentene, and *cis*-cyclooctene were purified in a similar manner by being washed with 1 M NaOH solution followed by  $\text{H}_2\text{O}$ , dried over anhydrous  $\text{Na}_2\text{SO}_4$ , distilled over powdered NaOH under a nitrogen atmosphere, and passed through neutral alumina before use. Norbornylene was purified by sublimation. The solvent  $\text{CH}_2\text{Cl}_2$  was of the highest purity, and its preparation has been described in a previous publication as Grade A.<sup>1d</sup> The HPLC and GC conditions have been previously described.<sup>1d</sup>

**Kinetic Methods.** All reactions have been studied in  $\text{CH}_2\text{Cl}_2$  solvent at 25 °C under a dry and oxygen-free atmosphere. Kinetic procedures have been described previously.<sup>1d</sup> Software based upon the method of Gear integration was employed in conjunction with a Vax 11/750 computer for the integration of integral equations arising from the kinetic schemes. The concentrations of reactants as a function of time were generated by this means.

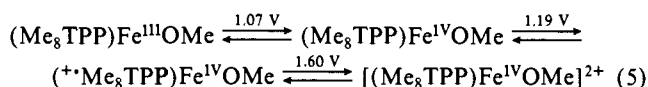
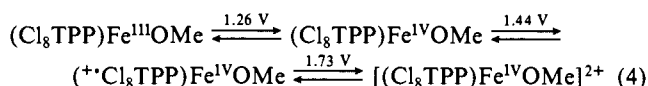
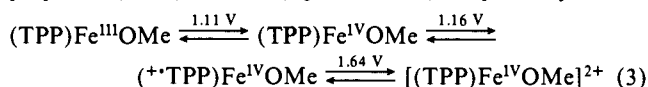
**Spectra and extinction coefficients** of products have been previously reported.<sup>1d</sup> Pertinent to this study are the following: *p*-cyano-*N,N*-dimethylaniline,  $\epsilon_{280} = 1.8 \times 10^4 \text{ M}^{-1} \text{cm}^{-1}$ ,  $\epsilon_{320} = 4.25 \times 10^3 \text{ M}^{-1} \text{cm}^{-1}$ ; *p*-cyano-*N*-methylaniline,  $\epsilon_{280} = 2.6 \times 10^4 \text{ M}^{-1} \text{cm}^{-1}$ ,  $\epsilon_{320} = 1.5 \times 10^3 \text{ M}^{-1} \text{cm}^{-1}$ ; *p*-cyanoaniline,  $\epsilon_{280} = 1.5 \times 10^4 \text{ M}^{-1} \text{cm}^{-1}$ ,  $\epsilon_{320} = 1.5 \times 10^2 \text{ M}^{-1} \text{cm}^{-1}$ ; *p*-cyano-*N*-formyl-*N*-methylaniline,  $\epsilon_{280} = 1.5 \times 10^4 \text{ M}^{-1} \text{cm}^{-1}$ ,  $\epsilon_{320} = 4.5 \times 10^2 \text{ M}^{-1} \text{cm}^{-1}$ ; *N,N'*-dimethyl-*N,N'*-bis(*p*-cyanophenyl)hydrazine,  $\epsilon_{280} = 3.5 \times 10^4 \text{ M}^{-1} \text{cm}^{-1}$ ,  $\epsilon_{320} = 4.2 \times 10^3 \text{ M}^{-1} \text{cm}^{-1}$ ; *N,N'*-bis(*p*-cyanophenyl)-*N*-methylmethylenediamine,  $\epsilon_{280} = 1.0 \times 10^4 \text{ M}^{-1} \text{cm}^{-1}$ ,  $\epsilon_{320} = 2.8 \times 10^3 \text{ M}^{-1} \text{cm}^{-1}$ .

## Results

The reaction of *meso*-(tetrakis(2,6-dimethylphenyl)porphinato)iron(III) chloride  $(\text{Me}_8\text{TPP})\text{Fe}^{\text{III}}\text{Cl}$  with *p*-cyano-*N,N*-dimethylaniline *N*-oxide (NO) yields *p*-cyano-*N,N*-dimethylaniline (DA), *p*-cyano-*N*-methylaniline (MA), *p*-cyanoaniline (A), *p*-cyano-*N*-formyl-*N*-methylaniline (FA), *N,N'*-dimethyl-*N,N'*-bis(*p*-cyanophenyl)hydrazine (H), *N,N'*-bis(*p*-cyanophenyl)-*N*-methylmethylenediamine (MD), and  $\text{CH}_2\text{O}$ . HPLC analysis of the reaction mixture at 280 and 320 nm showed complete material balance in both oxygen and nitrogen. In four separate experiments involving between 10 and 100 turnovers of catalyst ( $8.0 \times 10^{-5}$  M) the yields of the products DA, MA, A, FA, H, and MD were found to be 53%, 24%, 3%, 8%, 7%, and 5%, respectively (based upon initial  $[\text{NO}]_i$ ). The yield of  $\text{CH}_2\text{O}$  in each case is  $\sim 14\%$  (based on the method of Nash<sup>8</sup>).

The time course for the appearance of the collective products can be conveniently monitored spectrophotometrically at 320 nm where absorption by the metalloporphyrin is minimal. Changes in  $A_{320}$  with time (see Experimental Section) were found to follow the first-order rate law. Under the conditions of  $[\text{NO}]_i \gg$

potentials of hydroxide and methoxide ligated (tetraphenyl-, tetrakis(2,6-dichlorophenyl)-, and tetrakis(2,6-dimethylphenyl)-porphinato)iron(III) salts (eq 3, 4, and 5), respectively. Both



the electrochemical and the kinetics studies have been carried out at 25 °C in  $\text{CH}_2\text{Cl}_2$ . Comparison of the potentials of eq 3, 4, and 5 shows that  $(+\text{Cl}_8\text{TPP})\text{Fe}^{\text{IV}}\text{OMe}$  is a better oxidant than is  $(+\text{TPP})\text{Fe}^{\text{IV}}\text{OMe}$  by 280 mV, while the potential of  $(+\text{Me}_8\text{TPP})\text{Fe}^{\text{IV}}\text{OMe}$  is comparable to that of  $(+\text{TPP})\text{Fe}^{\text{IV}}\text{OMe}$ .

## Experimental Section

**meso**-(Tetrakis(2,6-dimethylphenyl)porphyrin)  $(\text{Me}_8\text{TPPH}_2)$  was synthesized by the procedure described by Zipples, Lee, and Bruce.<sup>3</sup> **meso**-(Tetrakis(2,6-dimethylphenyl)porphinato)iron(III) chloride  $(\text{Me}_8\text{TPP})\text{Fe}^{\text{III}}\text{Cl}$  was prepared from *meso*-tetrakis(2,6-dimethylphenyl)porphyrin and hydrated ferrous chloride according to the method of Kobayashi<sup>4</sup> and was characterized by  $^1\text{H}$  NMR,<sup>5</sup> UV-vis, and mass spectrometry.<sup>6</sup>  $^1\text{H}$  NMR ( $\text{CD}_2\text{Cl}_2$ )  $\delta$  3.86 (br s, 12 H), 6.56 (br s, 12

(3) Zipples, M. F.; Lee, W. A.; Bruce, T. C. *J. Am. Chem. Soc.* **1986**, *108*, 4433.

(4) Kobayashi, H.; Higuchi, T.; Kaizu, Y.; Osada, H.; Aoki, M. *Bull. Chem. Soc. Jpn.* **1975**, *48*, 3137.

(5) The  $^1\text{H}$  NMR spectrum obtained for  $(\text{Me}_8\text{TPP})\text{Fe}^{\text{III}}\text{Cl}$  is similar to that reported by Balch et al. for *meso*-(tetramesitylporphyrin)iron(III) chloride as one would expect for porphyrins with similar structural features (see: Cheng, R.-J.; Latos-Grazynski, L.; Balch, A. L. *Inorg. Chem.* **1982**, *21*, 2412).

(6) The mass spectrum was performed under the auspices of the Mass Spectral Facility at UCR under the direction of Professor C. L. Wilkins (NIH GM 30604).

(7) Woon, T. C.; Shirazi, A.; Bruce, T. C. *Inorg. Chem.* **1986**, *25*, 3845.

(8) Nash, T. *Biochem. J.* **1953**, *55*, 416.

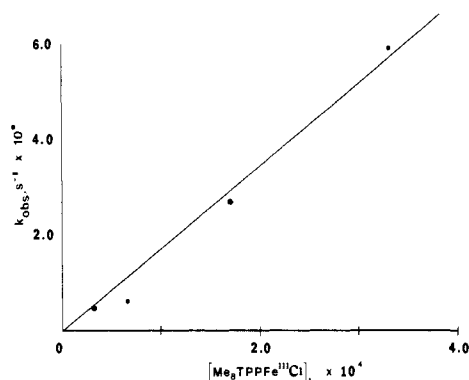


**Figure 3.** Plot of  $k_{\text{obsd}}$  vs.  $[(\text{Me}_8\text{TPP})\text{Fe}^{\text{III}}\text{Cl}]_i$  showing the linear dependence of  $k_{\text{obsd}}$  on the  $[(\text{Me}_8\text{TPP})\text{Fe}^{\text{III}}\text{Cl}]_i$  where the slope yields a second-order rate constant of  $\sim 1.7 \text{ M}^{-1} \text{ s}^{-1}$ .

**Table I.** Effect of [TBPH] on the Percentage Yields (based upon  $[\text{NO}]_i = 2.5 \times 10^{-3} \text{ M}$ ) of TBP\*, DA, and MA and on the Pseudo-First-Order Rate Constant for TBP\* Formation Monitored at 630 nm<sup>a</sup>

[TBPH] <sub>i</sub> , M	% yield of products			$k_{\text{obsd}}/[(\text{Me}_8\text{TPP})\text{Fe}^{\text{III}}\text{Cl}]_i$ , $\text{M}^{-1} \text{ s}^{-1}$
	DA	MA	TBP*	
0.03	88	12	88	1.67
0.15	90	10	90	1.07
0.30	93	7	93	0.67

<sup>a</sup>  $[(\text{Me}_8\text{TPP})\text{Fe}^{\text{III}}\text{Cl}]_i = 8.4 \times 10^{-5} \text{ M}$ .

$[(\text{Me}_8\text{TPP})\text{Fe}^{\text{III}}\text{Cl}]_i$  and at constant iron(III) porphyrin concentration the pseudo-first-order rates do not vary appreciably with changes in  $[\text{NO}]_i$ . The initial rate shows an increase with increase in  $[\text{NO}]_i$  (Figure 2). The pseudo-first-order rate constant for product formation is a linear function of  $[(\text{Me}_8\text{TPP})\text{Fe}^{\text{III}}\text{Cl}]_i$  as shown in Figure 3. The slope of Figure 3 provides the second-order rate constant ( $1.7 \text{ M}^{-1} \text{ s}^{-1}$ ) for reaction of NO with  $(\text{Me}_8\text{TPP})\text{Fe}^{\text{III}}\text{Cl}$ .

**The Time Course for the Formation of Each Product in the  $(\text{Me}_8\text{TPP})\text{Fe}^{\text{III}}\text{Cl}$  ( $1.0 \times 10^{-4} \text{ M}$ ) Catalyzed Decomposition of NO ( $2.8 \times 10^{-3} \text{ M}$ ).** Reactions were carried out under nitrogen, and aliquots were withdrawn under flowing nitrogen and stored in dry-ice chilled, gas-tight nitrogen-filled vials. Plots of concentration vs. time for products DA, MA, A, FA, H and MD (determined by HPLC analysis) are shown in Figure 4 (spectra A–F). The plots fitted to the experimental points represent best fits to the first-order rate law. The first-order rate constants for the formation of DA, MA, A, FA, H, and MD ( $2.9 \times 10^{-4}$ ,  $2.1 \times 10^{-4}$ ,  $3.0 \times 10^{-4}$ ,  $2.8 \times 10^{-4}$ ,  $2.6 \times 10^{-4}$ , and  $2.8 \times 10^{-4} \text{ s}^{-1}$ , respectively) may be compared to the spectrally determined first-order rate constant for the change in  $A_{320}$  with time ( $2.5 \times 10^{-4} \text{ s}^{-1}$ ) for this experiment.

**Oxidation of 2,4,6-tri-*tert*-butylphenol (TBPH) in the presence of NO catalyzed by  $(\text{Me}_8\text{TPP})\text{Fe}^{\text{III}}\text{Cl}$**  was followed at the  $\lambda_{\text{max}}$  of the phenoxyl radical (TBP\*) at 630 nm ( $\epsilon_{630} = 400 \text{ M}^{-1} \text{ cm}^{-1}$ ), and the percentage yields of products were determined at the completion of the reaction (Table I). Examination of Table I shows that the second-order rate constant for reaction of NO with  $(\text{Me}_8\text{TPP})\text{Fe}^{\text{III}}\text{Cl}$  (i.e.,  $k_{\text{obsd}}/[(\text{Me}_8\text{TPP})\text{Fe}^{\text{III}}\text{Cl}]_i$ ) decreases with increase in  $[\text{TBPH}]_i$ . TBPH traps  $\sim 90\%$  of the higher valent iron-oxo porphyrin species at all concentrations of TBPH employed and, thus,  $\sim 90\%$  DA and  $\sim 10\%$  MA are obtained for those reactions where the  $[\text{TBPH}]_i$  is between 0.03 and 0.30 M.

**A comparison of  $(\text{Me}_8\text{TPP})\text{Fe}^{\text{III}}\text{Cl}$  and  $(\text{Me}_8\text{TPP})\text{Fe}^{\text{III}}\text{OH}$**  as catalysts for the decomposition of NO was carried out. The objective of this experiment was to determine if water produced in the reaction in the presence of TBPH might slow the reaction by its ligation. The results of Table II show that this exchange of ligand has little effect on the kinetics of the reaction in the presence or absence of alkene.

**Varying  $[\text{NO}]$  ( $1.2 \times 10^{-3}$  –  $3.8 \times 10^{-3} \text{ M}$ ) at constant  $[(\text{Me}_8\text{TPP})\text{Fe}^{\text{III}}\text{Cl}]$  ( $1.0 \times 10^{-4} \text{ M}$ ) and [2,3-dimethyl-2-butene]**

**Table II.** A Comparison of the Relative Rate for Reaction of  $(\text{Me}_8\text{TPP})\text{Fe}^{\text{III}}\text{OH}$  and  $(\text{Me}_8\text{TPP})\text{Fe}^{\text{III}}\text{Cl}$  with NO in the Presence and Absence of Alkene<sup>a</sup>

compounds	$k_{\text{rel}}$	$k_{\text{rel}}$
		cyclohexene (1.0 M)
$(\text{Me}_8\text{TPP})\text{Fe}^{\text{III}}\text{Cl}$	1.0	1.0
$(\text{Me}_8\text{TPP})\text{Fe}^{\text{III}}\text{OH}$	1.2	0.8

<sup>a</sup>  $[(\text{Me}_8\text{TPP})\text{Fe}^{\text{III}}\text{Cl}]_i$  and  $[(\text{Me}_8\text{TPP})\text{Fe}^{\text{III}}\text{OH}]_i = 9.3 \times 10^{-5} \text{ M}$ .  $[\text{NO}] = 2.9 \times 10^{-3} \text{ M}$  and [cyclohexene] at 1.0 M.

**Table III.** Effect of Varying the Initial Concentration of NO on the Product Yields  $[(\text{Me}_8\text{TPP})\text{Fe}^{\text{III}}\text{Cl}]_i = 1.0 \times 10^{-4} \text{ M}$  in the Presence of 1.0 M 2,3-Dimethyl-2-butene

$[\text{NO}]_i$ , M	% yield of products			$k_{\text{obsd}}/[(\text{Me}_8\text{TPP})\text{Fe}^{\text{III}}\text{Cl}]_i$ , $\text{M}^{-1} \text{ s}^{-1}$
	DA	MA	TME-oxide	
$1.2 \times 10^{-3}$	96	5	100	1.8
$1.9 \times 10^{-3}$	101	4	104	1.2
$2.7 \times 10^{-3}$	102	2	103	1.1
$3.8 \times 10^{-3}$	103	3	97	1.6

**Table IV.** Results from Experiments Which Involve Competitive Trapping of  $(^+\text{Me}_8\text{TPP})\text{Fe}^{\text{IV}}\text{O}$  Intermediate by TME at 1.0 M and by TBPH at Varying Concentrations ( $[(\text{Me}_8\text{TPP})\text{Fe}^{\text{III}}\text{Cl}]_i = 8.0 \times 10^{-5} \text{ M}$ ;  $[\text{NO}]_i = 2.2 \times 10^{-3} \text{ M}$ )

$[\text{TBPH}]_i$ , M	percentage yields			
	DA	MA	TME-oxide	TBP* <sup>a</sup>
0.003	97	5	76	25
0.015	95	5	64	30
0.03	94	6	60	46
0.30	93	7	0	93

<sup>a</sup> The % yield of TBP\* (based upon  $[\text{NO}]_i$ ) listed in the table has been calculated from the maximum value of  $A_{630}$  observed during the time course of the reaction.

(1.0 M) has no effect on either the product yields or the pseudo-first-order rate constants, and at 1.0 M TME, TME-epoxide and DA are obtained as products in 100% yield based upon  $[\text{NO}]_i$  (Table III).

**Competitive experiments, in which TME (1.0 M) and TBPH ( $3 \times 10^{-3}$  to  $3 \times 10^{-1} \text{ M}$ ) compete as substrate** for the intermediate higher valent iron-oxo porphyrin species produced in the  $(\text{Me}_8\text{TPP})\text{Fe}^{\text{III}}\text{Cl}$  ( $8.0 \times 10^{-5} \text{ M}$ ) catalyzed decomposition of NO ( $2.2 \times 10^{-3} \text{ M}$ ), were monitored spectrophotometrically at the  $\lambda_{\text{max}}$  of the radical product TBP\* (630 nm). In all kinetic experiments  $A_{630}$  first increased and then decreased with time. The time course for the change of  $A_{630}$  was fitted to a program for two sequential first-order reactions ( $\text{TBPH} \rightarrow \text{TBP}^* \rightarrow \text{nonabsorbing at 630 nm}$ ) to provide the pseudo-first-order rate constants for the first ( $k_{\text{obsd1}}$ ) and second ( $k_{\text{obsd2}}$ ) reactions. Under the conditions of  $[\text{TBPH}]_i > [\text{NO}]_i$  the values of  $k_{\text{obsd1}} = k_{\text{obsd2}} = \text{about } 1 \times 10^{-4} \text{ s}^{-1}$  which is comparable to the turnover rate ( $1.3 \times 10^{-4} \text{ s}^{-1}$ ) for the reaction of NO with  $(\text{Me}_8\text{TPP})\text{Fe}^{\text{III}}\text{Cl}$  at the concentration of the latter employed in these experiments (Figure 5). Thus, formation of  $(^+\text{Me}_8\text{TPP})\text{Fe}^{\text{IV}}\text{O}$  is rate controlling in the oxidation of both TBPH and TBP\*. From Table IV, decrease in  $[\text{TBPH}]_i$  brings about a greater yield of TME-epoxide, and at  $[\text{TBPH}] = 0.3 \text{ M}$  and  $[\text{TME}] = 1.0 \text{ M}$  there is no detectable yield of TME-oxide. Thus, the  $1e^-$  oxidation of TBPH is greatly favored over the epoxidation of TME.

**The Reaction of NO ( $2.6 \times 10^{-3} \text{ M}$ ) with  $(\text{Me}_8\text{TPP})\text{Fe}^{\text{III}}\text{Cl}$  ( $1.0 \times 10^{-4} \text{ M}$ ) in the Presence of Various Alkenes.** As evidenced from the data in Table V, the yields of DA and epoxide increase and the yields of demethylation products decrease with increase in [alkene]. This is of course due to the epoxidation of alkene competing with the oxidation of DA. The presence of alkene has virtually no effect on the pseudo-first-order rate constant for DA appearance when one considers the difference in solvent composition brought about by the alkene addition. A comparison of the calculated percent yield of DA based on the final absorbance of the reaction corresponds reasonably well with the yield of epoxide.

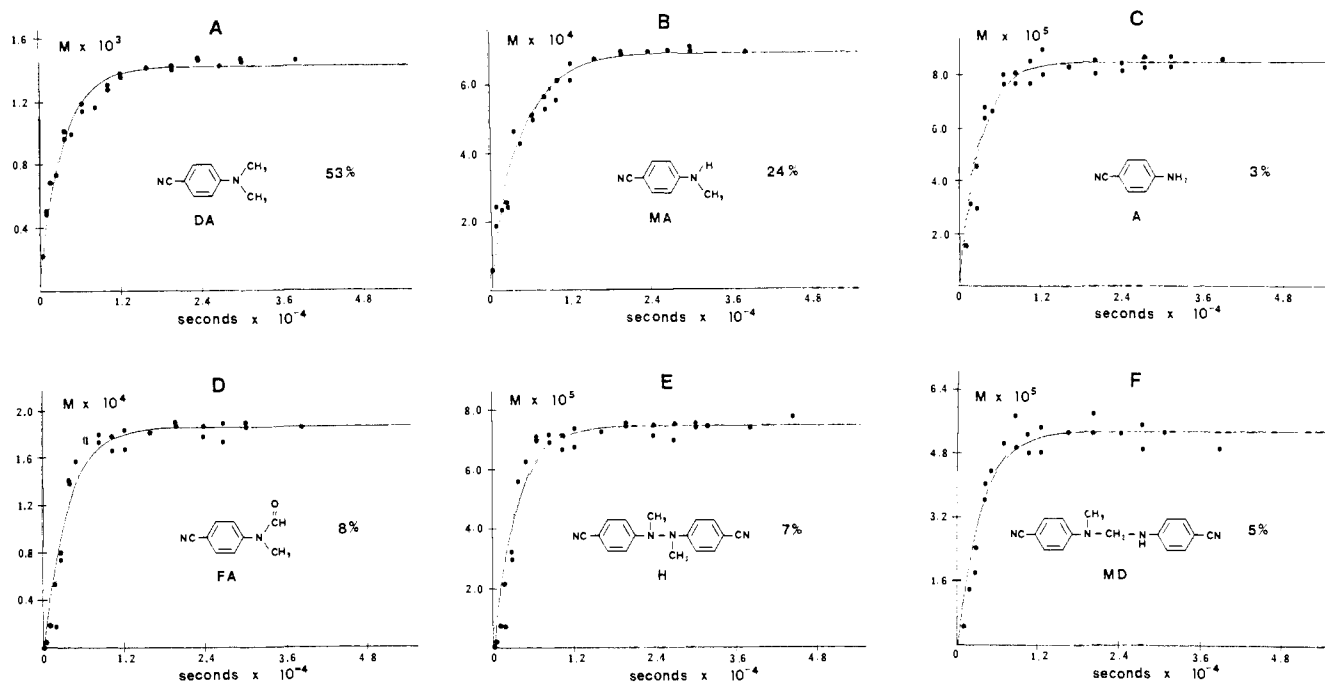


Figure 4. Plots of the time courses (determined by HPLC) for the products that are formed in first-order processes in the  $(\text{Me}_8\text{TPP})\text{Fe}^{\text{III}}\text{Cl}$  ( $1.0 \times 10^{-4}$  M) catalyzed decomposition of NO ( $2.8 \times 10^{-3}$  M).

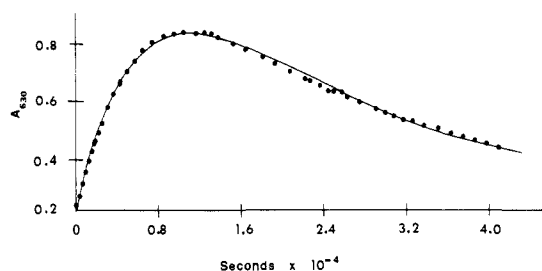


Figure 5. Plot of the time course for the change of  $A_{630}$  was fitted to a program for two sequential first-order reactions ( $\text{TBPH} \rightarrow \text{TBP} \rightarrow$  non-absorbing at 630 nm) to provide  $k_{\text{obsd1}} = k_{\text{obsd2}} = 1 \times 10^{-4} \text{ s}^{-1}$  at  $[(\text{Me}_8\text{TPP})\text{Fe}^{\text{III}}\text{Cl}] = 8.0 \times 10^{-5} \text{ M}$ ,  $[\text{NO}] = 2.2 \times 10^{-3} \text{ M}$ , and  $[\text{TBPH}] = 0.03 \text{ M}$ .

Increase in the concentration of these alkenes causes an increase in the yield of DA and epoxide with a subsequent decrease in the other products, MA, A, FA, H, and MD. At the same time the overall rate of the reaction remains about the same to within experimental errors (as shown in Table V).

**Repetitive scanning of the porphyrin Soret region (600–340 nm) during the  $(\text{Me}_8\text{TPP})\text{Fe}^{\text{III}}\text{Cl}$  ( $1.6 \times 10^{-4}$  M) catalyzed decomposition of NO ( $4.5 \times 10^{-3}$  M) revealed no spectral changes.** The scan speed was 480 nm/min with repetitive scans taken every 5 min to completion of the reaction. This result shows that the catalyst remains throughout the experiment overwhelmingly as the  $(\text{Me}_8\text{TPP})\text{Fe}^{\text{III}}\text{Cl}$  species. Thus, the catalyst is not saturated with NO (this feature being shown also by the pseudo-first-order nature of turnover kinetics) and there is no appreciable buildup of the higher valent iron-oxo species.

## Discussion

Evidence exists for dual cytochrome P-450 pathways for the N-demethylation of *N,N*-dimethylanilines. Pathway A involves aerobic demethylation catalyzed by a microsomal cytochrome P-450 system. Pathway B consists of two steps: N-oxidation of the tertiary amine by the oxygen dependent hepatic microsomal flavin mixed function oxidase and subsequent anaerobic demethylation of the *N*-oxide by a cytochrome P-450 with unusual properties.<sup>9</sup> In other experiments it has been shown,<sup>10</sup> however,

Table V. Effect of [Alkene] on the Product Yields and Relative Rate ( $k_{\text{rel}}$ ) in the  $(\text{Me}_8\text{TPP})\text{Fe}^{\text{III}}\text{Cl}$  ( $1.0 \times 10^{-4}$  M) Catalyzed Decomposition of NO ( $2.6 \times 10^{-3}$  M)

[alkene]	% yield of products							$k_{\text{rel}}^a$
	DA	MA	A	FA	H	MD	epoxide	
[cyclohexene], M								
0.0	60	10	2	4	7	8	0	1.0
0.01	58	11	0	4	7	6	26	0.9
0.1	74	12	0	0	4	4	70	1.3
1.0	97	2	0	0	0	0	100	3.0
[styrene], M								
0.0	58	9	5	4	6	6	0 <sup>b</sup>	1.0
0.1	94	0	2	2	5	2	98 <sup>b</sup>	2.0
1.0	104	2	0	0	0	0	102 <sup>b</sup>	1.25
[cyclopentene], M								
0.0	52	16	2	3	5	5	0	1.0
0.01	64	12	1	3	5	5	27	0.78
1.0	98	4	0	0	0	0	85	0.78
[cis-cyclooctene], M								
0.0	58	9	5	5	6	6	0	1.0
0.01	67	8	6	3	7	6	16	0.9
0.1	82	5	2	5	9	6	49	1.9
1.0	104	2	0	0	0	0	80	1.2
[norbornylene], M								
0.0	61	18	4	5	8	2	0	1.0
0.01	69	17	5	4	6	2	17	1.0
0.1	85	10	3	0	4	2	39	1.1
1.0	104	2	0	0	0	0	80	1.6

<sup>a</sup> Rate constant determined from the change of  $A_{320}$  with time relative to the rate constant in the absence of alkene. <sup>b</sup> Based upon the yields of DA. The percentage yields are for a mixture of styrene oxide (~80%) and phenylacetaldehyde (~20%).

that both cytochrome P-450<sub>LM</sub> and cytochrome P-450<sub>CAM</sub> catalyze the decomposition of substituted *N,N*-dimethylaniline *N*-oxides to *N*-methylanilines and  $\text{CH}_2\text{O}$  under anaerobic conditions.

The reasons for choosing *p*-cyano-*N,N*-dimethylaniline *N*-oxide (NO) with (tetraphenylporphinato)metal(III) salts as an oxygen donor molecule for oxygen transfer to organic substrates follow: (i) NO has some important advantages not yet found in any other single oxygen donor which include its solubility in polar solvents, monomeric nature, and lack of a propensity to oxidatively destroy the porphyrin ring in the absence of a substrate; (ii) epoxidation

(9) Hamill, S.; Cooper, D. Y. *Xenobiotica* 1984, 14, 139.

(10) Heimbrook, D. C.; Murray, R. I.; Egeberg, E. D.; Sliagar, S. G.; Nee, M. W.; Bruce, T. C. *J. Am. Chem. Soc.* 1984, 106, 1514.

and hydroxylation yields with NO as the oxygen source with the appropriate metalloporphyrin are equivalent to or higher than those obtained with such oxygen donor agents as PhIO, NaOCl, etc.; and (iii) NO serves as a double-reagent insofar that it carries out a 2e<sup>-</sup> oxidation of the metal(III) porphyrin and transfers an oxygen to the metal atom and also supplies *p*-cyano-*N,N*-dimethylaniline as an oxidizable substrate (eq 2). Such a double-reagent is highly useful in studies of the dynamics of the reactions, because the formation and oxidation of the *p*-cyano-*N,N*-dimethylaniline can be followed spectrophotometrically.

The reaction of *p*-cyano-*N,N*-dimethylaniline *N*-oxide (NO) with *meso*-(tetrakis(2,6-dimethylphenyl)porphinato)iron(III) chloride ((Me<sub>8</sub>TPP)Fe<sup>III</sup>Cl) (25 °C, CH<sub>2</sub>Cl<sub>2</sub> solvent, anaerobic) provides the following as products: *p*-cyano-*N,N*-dimethylaniline (DA), *p*-cyano-*N*-methylaniline (MA), *p*-cyano-*N*-formyl-*N*-methylaniline (FA), *p*-cyanoaniline (A), *N,N'*-dimethyl-*N,N'*-bis(*p*-cyanophenyl)hydrazine (H), *N,N'*-bis(*p*-cyanophenyl)-*N*-methylmethylenediamine (MD), and CH<sub>2</sub>O. The iron(III) porphyrin is not oxidatively consumed. The percentage yields of the products and the dynamics for DA, MA, FA, A, H, and MD formation have been determined at various concentrations of both NO and iron(III) porphyrin salt. Appearance of each product followed the first-order rate law to at least 7 × *t*<sub>1/2</sub>. Under the pseudo-first-order conditions of [NO]<sub>i</sub> > [(Me<sub>8</sub>TPP)Fe<sup>III</sup>Cl]<sub>i</sub>, the pseudo-first-order rate constant for the disappearance of NO is independent of the [NO]<sub>i</sub> but varies linearly with changes in the [(Me<sub>8</sub>TPP)Fe<sup>III</sup>Cl]<sub>i</sub>. The reaction is, therefore, first order in both [NO]<sub>i</sub> and [(Me<sub>8</sub>TPP)Fe<sup>III</sup>Cl]<sub>i</sub>. The second-order rate constant for reaction of NO with (Me<sub>8</sub>TPP)Fe<sup>III</sup>Cl was determined as ~1.7 M<sup>-1</sup> s<sup>-1</sup>. The rate of reaction of NO and (TPP)Fe<sup>III</sup>Cl (~5.5 M<sup>-1</sup> s<sup>-1</sup>) is 3.3-fold greater than the rate for reaction of NO and (Me<sub>8</sub>TPP)Fe<sup>III</sup>Cl. The small difference in the free energies of the two reactions (~0.65 kcal M<sup>-1</sup>) might be taken to reflect a small difference in the electron densities of the iron(III) moieties and a steric effect to the approach of reactants by the eight *o*-methyl substituents. Electron release by the methyl substituents does not, however, appear to be of any great significance as shown by the potentials of eq 3 and 5. It should be pointed out that rationalizations of such small rate ratios (ΔΔ*G*<sup>‡</sup> < 1.0 kcal M<sup>-1</sup>) are never secure. The yields of products DA, MA, FA, A, and H for the reaction of (Me<sub>8</sub>TPP)Fe<sup>III</sup>Cl and (TPP)Fe<sup>III</sup>Cl with NO are essentially identical. This reflects the similarity in the oxidation potential of the two derived iron(IV)-oxo porphyrin π-cation radical species.

The rate constants for the formation of each of the products DA, MA, A, FA, H, and MD are found to be the same. Since the cascade of oxidations involves, overall, DA → FA, DA → MA → A, 2MA → MD, and 2MA → H (formation of each product consuming one (\*Me<sub>8</sub>TPP)Fe<sup>IV</sup>O), the finding that all products arise with the same rate constant simply means that all of these oxidation steps are associated with rate constants which are much larger than that for the rate-determining oxygen-transfer step which provides (\*Me<sub>8</sub>TPP)Fe<sup>IV</sup>O. Thus, the experimentally determined rate constant for catalyst turnover (1.7 M<sup>-1</sup> s<sup>-1</sup>) is the rate constant for reaction of NO with (Me<sub>8</sub>TPP)Fe<sup>III</sup>Cl to provide (\*Me<sub>8</sub>TPP)Fe<sup>IV</sup>O. The dynamics for the reaction of NO with (Me<sub>8</sub>TPP)Fe<sup>III</sup>Cl, including the correct percentage yield of each product, may be computer-simulated by use of the same sequence of reactions employed<sup>1d</sup> for the computer-simulation of the reaction of (TPP)Fe<sup>III</sup>Cl with NO (Scheme I). The rate constants for the oxidation steps in the conversion of DA to MA, FA, H, A, and MD which were used in the computer simulation (Figure 4) are minimal values and are provided in Table VI.

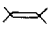
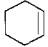
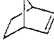
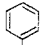


In a previous study, 2,4,6-tri-*tert*-butylphenol (TBPH) served well as a trap for the (\*TPP)Fe<sup>IV</sup>O species generated from (TPP)Fe<sup>III</sup>Cl with NO. Increasing the concentration of TBPH had no effect upon the rate constant for NO consumption. The use of TBPH with (Me<sub>8</sub>TPP)Fe<sup>III</sup>Cl and NO results in ~90% trapping of the iron(IV)-oxo porphyrin π-cation radical species. Increasing the initial TBPH concentration, however, brings about a slight decrease in the pseudo-first-order rate constant (Table I). This, of course, renders TBPH useless as a trapping reagent

**Table VI.** Minimal Rate Constants Employed To Fit the Experimental Points of Figures 4A–F (using Scheme I) Which Show the Time Course for the Formation of Each Product in the (Me<sub>8</sub>TPP)Fe<sup>III</sup>Cl (Initial Concentration = 8.0 × 10<sup>-5</sup> M) Catalyzed Decomposition of NO (Initial Concentration = 2.8 × 10<sup>-3</sup> M)<sup>a</sup>

<i>k</i> <sub>c</sub>	600.0 M <sup>-1</sup> s <sup>-1</sup>
<i>k</i> <sub>d</sub>	6.0 × 10 <sup>8</sup> M <sup>-1</sup> s <sup>-1</sup>
<i>k</i> <sub>e</sub>	600.0 M <sup>-1</sup> s <sup>-1</sup>
<i>k</i> <sub>f</sub>	1.0 × 10 <sup>5</sup> M <sup>-1</sup> s <sup>-1</sup>
<i>k</i> <sub>g</sub> / <i>k</i> <sub>-g</sub>	1.0 × 10 <sup>3</sup> /1.3 × 10 <sup>4</sup> M
<i>k</i> <sub>h</sub>	600.0 M <sup>-1</sup> s <sup>-1</sup>
<i>k</i> <sub>i</sub>	2.0 × 10 <sup>7</sup> M <sup>-1</sup> s <sup>-1</sup>
<i>k</i> <sub>j</sub>	6.0 × 10 <sup>8</sup> M <sup>-1</sup> s <sup>-1</sup>
<i>k</i> <sub>k</sub>	3.5 × 10 <sup>8</sup> M <sup>-1</sup> s <sup>-1</sup>
<i>k</i> <sub>l</sub>	3.0 × 10 <sup>3</sup> M <sup>-1</sup> s <sup>-1</sup>

<sup>a</sup> The experimentally determined value of 1.7 M<sup>-1</sup> s<sup>-1</sup> was used as *k*<sub>a</sub>*k*<sub>b</sub>/*k*<sub>-a</sub>.

**Table VII.** Comparison of Epoxide Yields (based upon [NO]<sub>i</sub>) with Three (Tetrakis(2,6-disubstituted phenyl)porphinato)iron(III) Chlorides (Alkenes at 1.0 M)

alkenes	(Cl <sub>8</sub> TPP)Fe <sup>III</sup> Cl <sup>1c</sup>	(TPP)Fe <sup>III</sup> Cl <sup>1d</sup>	(Me <sub>8</sub> TPP)Fe <sup>III</sup> Cl
	25	100	100
	34	45	100
	0	36	80
			100
			85
			80

to provide an alternate confirmation of the rate constant for the commitment step of oxygen transfer from N → Fe<sup>III</sup>.

The addition of alkenes (2,3-dimethyl-2-butene, cyclohexene, styrene, cyclooctene, cyclopentene, and norbornylene) to the (Me<sub>8</sub>TPP)Fe<sup>III</sup>Cl catalyzed decomposition of NO has little effect on the kinetics of the reaction. This result establishes that epoxidation is not at all rate determining. The product yields in the presence of alkenes reflect what is to be expected for alkene epoxidation by (\*Me<sub>8</sub>TPP)Fe<sup>IV</sup>O (Table V). The higher the olefin concentration is the higher the corresponding epoxide yield is, and, therefore, the DA yield increases while the yields of MA, A, FA, H, and MD decrease. Since the (\*Me<sub>8</sub>TPP)Fe<sup>IV</sup>O species is being used up by epoxidation of alkene, it is no longer able to oxidize DA in any appreciable amount to MA (see Scheme I).<sup>1d</sup> *p*-Cyano-*N*-methylaniline (MA) is the intermediate in the formation of A, H, and MD; with MA being produced in lower yields, the yields of A, H, and MD must decrease as well. The 1e<sup>-</sup> oxidations of 2,4,6-tri-*tert*-butylphenol, DA, and MA are associated with rate constants which are much greater than those for olefin epoxidation.

At 1.0 M alkenes, the only products are DA (>90%) and MA (<10%) and the respective epoxides. The percent yield of the epoxides when employing (TPP)Fe<sup>III</sup>Cl, (tetrakis(2,6-dichlorophenyl)porphinato)iron(III) chloride ((Cl<sub>8</sub>TPP)Fe<sup>III</sup>Cl), and (Me<sub>8</sub>TPP)Fe<sup>III</sup>Cl are compared in Table VII. Inspection of Table VII shows that electron removal from the porphyrin ligand results in a poorer catalyst for epoxidation. Two types of reactions are in competition. These are epoxidation and oxidation of DA and its oxidation product MA (Scheme I). As the porphyrin becomes more electron deficient the oxidation of DA and MA is favored over epoxidation. Thus, when (tetrakis(pentafluorophenyl)porphinato)iron(III) chloride ((F<sub>20</sub>TPP)Fe<sup>III</sup>Cl) is used with NO, epoxidation of olefins can scarcely compete at all with the amine oxidations.<sup>11</sup> The ratio of the second-order rate constants

(11) Ostovic, D.; Bruce, T. C., unpublished results.

$[k_{\text{obsd}}/((\text{porphyrin})\text{Fe}^{\text{III}}\text{Cl})]$  for reaction with NO are in the order  $(\text{Me}_8\text{TPP})\text{Fe}^{\text{III}}\text{Cl}:(\text{TPP})\text{Fe}^{\text{III}}\text{Cl}:(\text{Cl}_8\text{TPP})\text{Fe}^{\text{III}}\text{Cl} = 1:3:235$ . There are two conclusions to be drawn: (i) the more electron deficient the iron(III) porphyrin moiety is the greater the rate constant for oxygen transfer from NO to the ligated iron(III) is and (ii) demethylation of *N,N*-dimethyl- and *N*-methylanilines is more sensitive to the electronic nature of the iron(IV)-oxo porphyrin  $\pi$ -cation radical than is epoxidation, though the rate constants for both processes must increase with a decrease in the electron density of the higher valent iron-oxo species.

**Conclusion.** The immediate products of the reaction of  $(\text{Me}_8\text{TPP})\text{Fe}^{\text{III}}\text{Cl}$  with NO are DA and a higher valent iron-oxo porphyrin which, on the basis of other studies,<sup>2</sup> can be assigned the structure of an iron(IV)-oxo porphyrin  $\pi$ -cation radical  $(^+\text{Me}_8\text{TPP})\text{Fe}^{\text{IV}}\text{O}$ . Reaction of 1 and 2 equiv of the latter with DA provides MA and FA, respectively, and its further involvement in the oxidation of MA yields MD, H, and A. Under the pseudo-first-order conditions of  $[\text{NO}]_i \gg [(\text{Me}_8\text{TPP})\text{Fe}^{\text{III}}\text{Cl}]_i$ , each of the products DA, MA, FA, MD, H, and A appear with the same pseudo-first-order rate constant. Two inevitable conclusions can be reached: (i) ligation of NO to the catalyst  $(\text{Me}_8\text{TPP})\text{Fe}^{\text{III}}\text{Cl}$

does not involve saturation of the latter, and (ii) the rate-determining step involves oxygen transfer from  $\text{N} \rightarrow$  iron(III) within the  $\text{Me}_8\text{TPP}(\text{Cl})\text{Fe}^{\text{III}}\text{ON}$  complex to provide DA and the higher valent iron-oxo porphyrin. Epoxidation yields with six alkenes (at 1.0 M) range between 100% and 80% (based upon the initial concentration of NO) when using  $(\text{Me}_8\text{TPP})\text{Fe}^{\text{III}}\text{Cl}$  as catalyst. The epoxidations are not rate-controlling. The use of NO with  $(\text{Me}_8\text{TPP})\text{Fe}^{\text{III}}\text{Cl}$  provides a very mild method for alkene epoxidation in high yields. By use of the sterically hindered  $(\text{Me}_8\text{TPP})\text{Fe}^{\text{III}}\text{Cl}$  there is prevented the reaction of  $[(\text{Me}_8\text{TPP})\text{Fe}^{\text{III}}]^+$  with  $(^+\text{Me}_8\text{TPP})\text{Fe}^{\text{IV}}\text{O}$  to yield  $[(\text{Me}_8\text{TPP})\text{Fe}^{\text{IV}}]_2\text{O}$ . Complications of kinetic interpretations by such a reaction have been considered by Nolte and associates.<sup>12</sup>

**Acknowledgment.** This work was supported by grants from the National Institutes of Health and the National Science Foundation.

(12) Nolte, R. J. M.; Razenberg, J. A. S. J.; Schurman, R. J. *Am. Chem. Soc.* **1986**, *108*, 2751.

## Dimerization Energetics of Benzene and Aromatic Amino Acid Side Chains

S. K. Burley\*<sup>†,§</sup> and G. A. Petsko<sup>†</sup>

Contribution from the Department of Chemistry Massachusetts Institute of Technology, Cambridge, Massachusetts 02139, and Harvard Medical School, Health Sciences and Technology Division, Boston, Massachusetts 02115. Received April 22, 1986

**Abstract:** Interactions between aromatic side chains in protein crystal structures have been studied by geometric analysis and nonbonded interaction energy calculations, based on ab initio quantum mechanical calculations of dibenzene. Aromatic side chains in proteins pair with preferred centroid separations of between 3.4 and 6.5 Å. Eighty-four percent of these aromatic pairs make enthalpically favorable edge-to-face interactions, which bring a  $\delta(+)$  hydrogen atom of one aromatic ring near to the  $\delta(-)$   $\pi$ -electron cloud of the other aromatic ring. The distribution of observed interaction geometries differs substantially from random and depends critically on the spatial arrangement of the two aromatic rings. These data demonstrate that the edge-to-face interaction of two aromatic side chains makes an enthalpic contribution of between -1 and -2 kcal/mol to the energy stabilization of a protein and does not arise solely as a function of packing constraints.

Recent surveys of aromatic side chain environments in single-crystal peptide structures and in protein crystal structures have documented statistically preferred interaction geometries between aromatic rings and neighboring atoms such as carbonyl oxygens, sulfurs, and amino groups.<sup>1-4</sup> In addition, Thomas et al.<sup>2</sup> used ab initio calculations to demonstrate that an enthalpically favorable interaction between the  $\delta(+)$  hydrogen atoms of aromatic side chains and the  $\delta(-)$  carbonyl oxygen atoms is responsible for their preferred interaction geometry, observed in protein and peptide crystal structures.

Edge-to-face packing of crystalline aromatic compounds was first appreciated in single-crystal structures of benzene<sup>5</sup> and its derivatives.<sup>6</sup> Such arrangements bring a  $\delta(+)$  hydrogen atom of one aromatic group into close contact with the  $\delta(-)$   $\pi$ -electron cloud of the other aromatic ring and are energetically favorable.<sup>7,8</sup> Similar arrangements of aromatic groups have been detected in surveys of aromatic side-chain environments of proteins by Burley and Petsko<sup>9</sup> and Singh and Thornton.<sup>10</sup> The present investigation extends these analyses by using the results of ab initio calculations of benzene dimerization to further characterize interactions be-

tween pairs of neighboring aromatic side chains in protein crystal structures.

### Procedures

**Geometric Analysis.** Thirty-three high-resolution ( $<2$  Å), refined protein crystal structures were examined for aromatic side chains near one another. Their packing geometry was analyzed with use of a right-handed polar coordinate system, which places the center of mass of one of the two six-membered rings, the reference ring, at the origin. Its 6-fold symmetry axis is colinear with the  $z$  axis, and the  $\text{C}_\beta\text{-C}_\gamma$  bond

(1) Gould, R. O.; Gray, A. M.; Taylor, P.; Walkinshaw, M. D. *J. Am. Chem. Soc.* **1985**, *107*, 5921.

(2) Thomas, K. A.; Smith, G. M.; Thomas, T. M.; Feldman, R. J. *Proc. Natl. Acad. Sci. U.S.A.* **1982**, *79*, 4843.

(3) Reid, K. S. C.; Lindley, P. F.; Thornton, J. M. *FEBS Lett.* **1985**, *190*, 209.

(4) Burley, S. K.; Petsko, G. A. *FEBS Lett.* **1986**, *203*, 139.

(5) Cox, E. G.; Cruickshank, D. W. J.; Smith, J. A. S. *Proc. R. Soc. London* **1958**, *247*, 1.

(6) Wyckoff, R. W. G. *Crystal Structures, The Structure of Benzene Derivatives*; Interscience: New York, 1969, Vol. 6.

(7) Karlström, G.; Linse, P.; Wallqvist, A.; Jonsson, B. *J. Am. Chem. Soc.* **1983**, *105*, 3777.

(8) Pawliszyn, J.; Szczesniak, M. M.; Scheiner, S. *J. Phys. Chem.* **1984**, *88*, 1726.

(9) Burley, S. K.; Petsko, G. A. *Science* **1985**, *229*, 23.

(10) Singh, J.; Thornton, J. M. *FEBS Lett.* **1985**, *191*, 1.

(11) Steed, J. M.; Dixon, T. A.; Klemperer, W. J. *J. Chem. Phys.* **1979**, *70*, 4940.

\* Author to whom correspondence should be addressed.

<sup>†</sup> Massachusetts Institute of Technology.

<sup>§</sup> Harvard Medical School.